

Bansilal Ramnath Agarwal Charitable Trust's VISHWAKARMA INSTITUTE OF TECHNOLOGY, PUNE – 411037.

(An Autonomous Institute Affiliated to Savitribai Phule Pune University, Pune.)



Major Project Report
Design, Fabrication & Control of an Ornithopter
Guided By
Prof. S. Pavitran
Presented By
B.Tech. Mechanical
Year 2021-2022

Name	Div	Roll No.	Gr. No.
Dhiren Bhabad	ME A	19	11810572
Ojas Mandlecha	ME C	22	11810880
Sankalp Gharmalkar	ME B	08	11810519
Shreeya Gadgil	ME A	68	11810511

CERTIFICATE

This is to certify that the project entitled "**Design, Fabrication and Control of an Ornithopter**" by students Vishwakarma Institute of Technology, Pune as a 40EDI project of 6th sem for session 2020-2021 is a bonafide record of project carried out by us under the supervision and guidance of PROF. (DR.) S. PAVITRAN, Department Of Mechanical Engineering.

The project is real and has not been submitted to any other university.

DATE: 30 / 06 /2022

Place: Vishwakarma Institute of Technology

Prof S. PAVITRAN

ACKNOWLEDGEMENT

The objective of this project is to provide a clear and thorough presentation of theory and practical knowledge of Amphibious robots.

To achieve this objective , the group members by no means have worked alone as these ideas have been shaped by comments, suggestions and acceptance given by **Prof. (Dr) S. PAVITRAN**, Department of Mechanical Engineering .

We are thankful to **Prof. (Dr) S. PAVITRAN** for his guidance, support and inputs in this course project without which it wouldn't have been a success.

We express our sincere thanks to the management of Vishwakarma Institute of Technology, Pune for allowing us to carry out such educational projects.

We express our feelings and respect towards our parents, without their blessings, help and motivation this project could not have been completed and would have been just a dream for us.

We are thankful to all those whom we might have inadvertently failed to mention here but have a positive contribution in successful completion of this project.

Special thanks to Instrumentation students, Shivangi Deo and Neeraj Sahasrabudhe as well as Aniruddha Atre of Mechanical Department for their valuable contribution and suggestions.

Group Members

Dhiren Bhadbod

Ojas Mandlecha

Sankalp Gharmalkar

Shreeya Gadgil

Index

ABSTRACT	6
Introduction	7
Lift Theories in birds	7
Literature Review	8
Methodology	12
Wing Dimensions	12
Torque Calculations:	13
BLDC Motor Torque	13
Servo Motor Torque calculation for Tail	14
Gearbox Calculations:	15
Design	19
Gearbox	19
Frontal pivot mechanism	20
Back pivot	20
Tail Mechanism	20
Final CAD	21
Analysis	21
Bearing Housing	21
Material: ABS	21
Material Properties	21
Boundary Conditions	22
Results	22
I. Total Deformation	22
II. Equivalent Stress	23
2. Rod Connecting Link	23
Material: ABS	23
Material Properties	23
Boundary Conditions	24
Results	24
I. Total Deformation	24
II. Equivalent Stress	25
3. Crank	25
Material: ABS	25
Material Properties	25
Boundary Conditions	26
Results	26
I. Total Deformation	26

II. Equivalent Stress	27
4. Rod	27
Material: SS	27
Material Properties	27
Boundary Conditions	28
Results	28
I. Total Deformation	28
II. Equivalent Stress	29
Wing Flexibility	29
Materials	29
Manufacturing Processes	30
Electronics	30
Components	30
Arduino UNO:	30
Transceiver module NRF24L01	31
Battery	32
Electronic Speed Control	32
BLDC Motor	33
Servo Motor	34
Joystick Module	34
Algorithm	35
Test Setup	35
Initial test setup:	35
Final phase test setup:	36
Challenges faced	37
Advantages of Ornithopter over drones	37
Future Scope:	38
Applications:	38
Conclusion:	38

ABSTRACT

The objective for this project is to design and implement an ornithopter capable of short-distance flight. An ornithopter is a robot that flies in a manner similar to a bird by generating flapping wing motion. Ornithopters can be more efficient, cost effective and environmentally friendly in comparison to fixed-wing aircrafts. This ornithopter has been designed considering a suitable mechanism using gearbox for flapping of the wings. The desired purpose of this ornithopter is stable flight using lift force and forward thrust generated using flapping of the wings. The prime mover here for the flapping mechanism is the BLDC motor. The gearbox is designed using optimum reduction of 22.8, so that it would provide sufficient torque and rpm both. 2 test setups were used to find the ornithopter can generate enough lift and thrust. The second test setup that included suspending the ornithopter using a rope proved that the ornithopter generated enough lift force as well as propelled forward.

I. Introduction

The definition of biomimetics as described by Raz Jelinek in his book Biomimetics is as follows: “the examination of nature, its models, systems, processes, and elements to emulate or take inspiration from in order to solve human problems.” Using this concept, the ornithopter was inspired by bird anatomy and behavior as well as physical principles of aerodynamics and mechanics. An ornithopter is a machine that flies by flapping its wings. Ornithopters are mainly meant to imitate bird flying. Ornithopters are often created to the same scale as their living counterparts. This span can range from hummingbird sized Nano Aerial Vehicles (NAVs) to ornithopters with wingspans that are large enough to carry human passengers. Flapping and occasionally airfoil wings are used by ornithopters to generate enough lift to bear their own weight. This method entails diverting air downward and creating pressure differences. Flapping must be combined with forward velocity to create lift force, allowing the ornithopter to fly. Unlike traditional aircrafts such as commercial jets, which use turbines and fans to generate thrust, ornithopters generate thrust by flapping wings. On the other hand, both commercial jets and ornithopters use their wing shape as well as their angle of attack to provide lift that in turn, keeps them in the air. The flapping wing design offers many benefits, including improved efficiency, better maneuverability and reduced noise compared to traditional fixed wing and rotary aircrafts. Most ornithopters are built for leisure, but research into imitating the biological systems of birds could lead to significant advancements in the aircraft industry. Some advancements include goods in the military, scientific, and commercial sectors, which would most likely lead to a new optimal solution for air travel. Ornithopter wing test beds, models, and research have served as motivation for developing an electronically driven ornithopter that can be controlled remotely and wirelessly. Ornithopters can be employed by researchers to conduct more in-depth wildlife studies, as well as by the commercial industry for payload transportation. Ornithopters can also be used for surveillance and are used in a variety of military applications. They are advantageous in this industry because they have a low aero-acoustic signature, or machine noise. Furthermore, due to their aerodynamic qualities, ornithopters are appropriate small scale aerial vehicles. Although small ornithopters are vulnerable to wind gusts, they have the ability to do challenging maneuvers such as hovering and backward flight. Ornithopter pioneers have determined that these devices have a wide range of potential contributions to the science of aerial remote sensing.

A. Lift Theories in birds

Simple flapping of an ornithopter's wings with well chosen parameters and an overall lightweight design is capable of creating the necessary lift and push to allow the device to carry its own weight and fly. Birds use a variety of techniques to change the vertical flapping motion that they may create. Larger birds with slow flapping rates have more stable aerodynamics than smaller birds with severely unstable or nonlinear flight. Due to an increasing viscous flow regime, smaller birds must work more to form vortices. Flapping can be divided into three separate

motions. For starters, flapping generates the most power and the greatest degree of freedom. Second, there's feathering or pitching, which is a pitching motion that varies along the length of the wings. Finally, lead lag is the lateral movement of the wings in-plane. The flapping axis, pitching axis, and lead lag are sometimes known as roll, pitch, and yaw. Flapping entails two strokes: upstroke and downstroke. During downstroke, the whole aerodynamic force is tilted, generating lift and push. The angle of attack is positive near the root and can be positive or negative towards the tip depending on how the wing pitches up. During the upstroke, the upper half of the wing generates an upward aerodynamic force with a backwards tilt, resulting in positive lift and negative thrust. The outer section of the wings produce positive lift and drag when the angle of attack is positive. When the angle of attack is negative, the wings provide negative lift and positive thrust.

II. Literature Review

Ornithopters have been a relatively obscure area of research in comparison to fixed wing aircraft and the field of ornithopter design is sparsely populated. Much of the research done has been performed by hobbyists such as Sean Kinkade[1]. Kinkade is the designer of a wide range of radio controlled ornithopters both smaller and larger than the Park Hawk that the Kestrel is based on and holds a patent on the design. Even though these machines have been designed both the ornithopters and plans are exceedingly hard to obtain. Both original designs and designs that build on Kinkade's that build are in progress in the hobbyist community but very little work has been published. Ornithopter designs in similar form factors that focus on adding additional degrees of freedom to the wings have been published in addition to a variable amplitude wing design produced by the Robot Locomotion Group previously. [2]

An extensive analysis of the wing design used here has been performed with a motion capture system by Robyn Harmon of the Morpheus Lab at the University of Maryland[3] which explains many of the aerodynamic properties of this type of ornithopter. The Morpheus Lab has also been working with the simple kinds of ornithopter control presented here. Paralleling this work similar results have been shown by the University of Arizona working with a 74cm wingspan ornithopter. Both of these projects make use of a very limited onboard computer in order to be lightweight enough to fly. James Delaurier's work forms much of what has been accomplished in larger scale ornithopter design and analysis. A project to build a piloted ornithopter has been ongoing for many years and achieved several seconds of sustained flight.

Dymytro Silin[4] studied the effects of wing loading, wing length and stroke amplitude were studied in tailless ornithopters. The flapping frequency and angle of attack required for level flight increased with wind loading. Variation of f with airspeed demonstrated a local minimum, which was hypothesized to correspond to the minimum power to fly. Required f and α decreased with wing length and stroke amplitude. The performance model of an ornithopter with tail and

fuselage was used to examine the effect of horizontal tail area and inclination angle. It was observed that decreasing the tail area allowed a decreased minimum flight speed with flapping frequency kept constant. Increasing the tail inclination angle allowed to increase maximum flight speed.

In 2014-2015, “Ornithopter Testbed to Discover Forces Produced by Flapping Wing Movement” [5] by Carlos Berdeguer, Hanna Schmidtman, and Austin Waid-Jones describes how flapping wing patterns can be used to optimize ornithopter designs. The team created a test bed that can be modified to find the wing strokes that allow for the most efficient flight. The system uses a four bar linkage that is modular to allow for varying patterns of motion. The modularity of the system is dependent on a protractor style of design with slots at various locations in place of one of the bars, which allows the linkages to be adjusted. Three motion patterns were studied by the members in this group. The motions consisted of a teardrop shape, a figure eight, and an almost linear pattern. These patterns are only a few examples that can be created using the linkage system, with many more existing options that could be implemented.

“Theoretical Model and Test Bed for the Development and Validation of Ornithopter Designs” [6] by Alexandra Beando, Christopher Overton, Tyler Pietri, Jesus Chung, and Kevin Ramirez analyzed the optimization of a linear flapping wing pattern. This testbed analyzed the performance of a prototype and devised guidelines for future iterations of ornithopters. One such recommendation was to implement a model that was lighter and had reduced friction. Their hole pattern, which involved drilling out small sections of the chassis without compromising structural stability, can be applied to ornithopters in order to reduce weight.

“Design and Construction of an Autonomous Ornithopter”[7] by Zachary John Jackowski documents the process of creating an ornithopter for research purposes. Jackowski, a student at MIT, documents the process that he undertook to create an ornithopter from scratch. The goals of Jackowski’s project was to create an autonomous ornithopter that could help to improve understanding of flapping wing flight. Jackowski’s ornithopter was designed for survivability and to be able to hold a large payload of sensor equipment. This ornithopter was named Phoenix and used rigid wings as opposed to jointed wings. The model was constructed with heavy, yet durable components.

Defining the primary wing’s size and shape is obtained from processing five steps of mission and flight status analysis, plan form and aspect ratio election, constraint analysis in order to calculate wing loading parameter, and finally weight estimation. In addition, with utilizing mentioned laws, essential parameters for designing fluttering mechanisms consist of flutter frequency, stroke angle, and advance ratio can be achieved. Needless to say that with having wingspan, wing area, and wing shape, along with fluttering parameters, initial flapping wings can be designed.

Modified Strip Theory[8] based on blade elemental analysis was used to develop the aerodynamic model for semi-elliptical wing form. Parametric study has been carried out to show the effect of different parameters on lift, thrust and drag forces for better understanding of ornithopter flight. Although there are endless possibilities of varying the inputs and getting the results in different forms but effect of only a few variable design parameters has been presented here for fixed size and geometry of wings for an ornithopter. It can be concluded from this study that:-

- a. Lift of an ornithopter is most influenced by the incidence angle and forward speed but least affected by flapping frequency.
- b. Thrust of an ornithopter is most affected by flapping frequency and forward speed but least influenced by incidence angle.
- c. The drag force increases with increase in forward speed, incidence angle, and flapping frequency.
- d. The increase in total flapping angle, increases all the forces but the effect is marked on drag force

Historically, aerodynamics of flapping wings was studied first on insects and birds, and steady flow assumption was quickly found inappropriate for the analysis of a flapping wing. Steady flow models failed to predict performance of a flapping wing because the unsteadiness of a flow around an oscillating wing was neglected. Some of the earliest studies in flapping flight aerodynamics implemented the quasi-steady approach to model insect flight. According to the quasi-steady assumption, motion of a flapping wing is analyzed at the set of fixed positions. Instantaneous velocity and aerodynamic forces are estimated in several cross sections using blade element theory. Then, forces acting on every element and at every position are integrated. Studies by Osborn, Jensen, and Weis-Fogh had shown limited success, because stroke-average lift of a flapping wing was underpredicted with quasi-steady assumption. Other approaches to characterize aerodynamics of a flapping wing include implementation of actuator disk/moment theory.[8]

The similarity between flapping wings and propellers was observed, giving an argument for an application of disk actuator theory to flapping-wing animals. The classical actuator disk theory provides an understanding of the performance of rotors, propellers, and ducted fans, and relates their performance to simple design parameters.

In the actuator disk theory, originally developed by Rankine and Froude[10], the disk axis of rotation is placed at the zero angle of attack with respect to the free stream. Applying the momentum theorem to a control volume surrounding the disk, the analytical relation was established between the wake velocity and thrust force generated by a given induced power to

the actuator. The zero angle of attack constraint may be applicable to vertical flights or hovering for.

Glauert et al [11]extended the actuator disk theory for a general flight case of the arbitrary angle of attack. Ellington et al modified the actuator disk theory by introducing a model of the partial actuator disk, which is obviously a better model for flapping wings that has a flapping amplitude less than 180 degrees.

In this model the disk area is defined as a projection of the area swept by flapping wings on the horizontal plane. Since the Rankine-Froude [12] theory assumes a uniform and continuous velocity distribution at any cross section of the control volume, the original theory was further modified by including non-uniform pressure distributions. Such modification was applied to a hovering flight, providing a spatial correction to the theory. A temporal correction to the actuator disk theory was developed by introducing pressure pulsations of frequency equal to the frequency of flapping. These two modifications were combined in one correction factor, which was eventually applied to the induced velocity and power in statically thrusting flapping wings. It was shown that this correction factor must be greater than unity. Willmot and Ellington used this correction to the wake velocity in a model for the mean lift coefficient and associated power components in insects in horizontal flight.

Overall, actuator disk theory is a relatively simple analytical treatment of the propulsive thrust and power. So far, substantial quantitative data have been obtained by applications of the theory to flying insects and birds. However, these data suffer uncertainties inherent to experiments on flying species. The unsteadiness of the flow around a flapping wing is caused by the flapping and rotation of a wing. The quasi-steady approaches provide integral solutions such as total lift or velocity in the far away wake but cannot predict local effects of pulsing and rotation of the flow around a flapping wing. Eventually, a number of aerodynamic mechanisms were proposed to explain generation of forces by a flapping wing.

In certain reviews the aerodynamics of flapping wings was presented as a combination of several complex phenomena, including: Wagner effects, wake capture, leading edge vortex, clap and fling, near fling, and apparent mass. Another important aspect of the flapping wing aerodynamics is a wing-air flow interaction. Evolution of birds and insects has brought about very sophisticated aerodynamic mechanisms, which are based on the natural flexibility of a flapping wing.

Reviews by Sane et al[14] and Ellington et al had [13] shown importance of passive and active deformations of a flapping wing on its lift generation and control capabilities In early works by Dalton and Ellington, the aerodynamic significance of wing deformations during flapping cycle was recognized, however, no detailed analysis of the phenomena was provided.

In one study, the wing kinematics in dragonflies was measured using a method of projected laser fringes, and recording their distortion with a high-speed camera. Deformations of wing camber

were observed, varying from positive camber (0.08-0.12) during downstroke to a negative camber of 3-4 times smaller magnitude and of relatively short duration on the upstroke. Based on two-dimensional unsteady CFD simulations performed on the stiff flat plate and on the airfoil with a time varying camber, importance of camber for lift generation was shown.

III. Methodology

A. Wing Dimensions

The concept of wing loading has been used to determine the wing surface area. Wing loading is the ratio of body weight to wing area. There is a standard relation between the weight of the flying object and its wing loading. In our case, considering the components to be used the mass of the ornithopter was assumed to be 0.75 kg and the corresponding wing loading is 60. Therefore, the wing area came out to be 0.13 m^2 .

$$\text{Wing loading} = \frac{\text{Body Weight}}{\text{Wing Area}}$$

$$30 = \frac{0.75 * 9.8}{\text{Wing Area}}$$

$$\text{Wing Area} = 0.26 \text{ m}^2$$

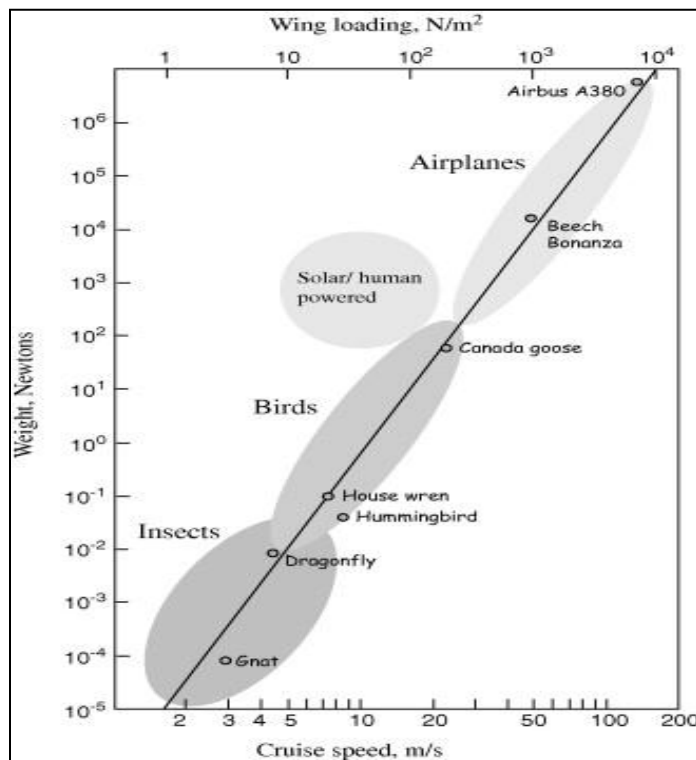


Figure1: Weight Vs Wing Loading [15]

B. Torque Calculations:

a. BLDC Motor Torque

To execute the flapping mechanism of the bird a mechanism similar to the slider-crank mechanism was chosen. To actuate the mechanism a BLDC motor was chosen as it is very light in weight as compared to other DC motors and with proper reduction ratio, appropriate torque and speed can be achieved. The BLDC motor transfers its energy through the gearbox to the crank to connect the rod to wings. Therefore the forces which act on the wings will decide the required torque for the BLDC motor. The major forces acting on the wings are the drag forces and their own weight. The drag force is calculated using the following formula.

$$Fd = 1/2 \times Cd \times Q \times A \times V^2$$

The required area of the wing calculated above and the shape of the wing which closely resembles a semi-ellipse help us narrow it down to dimension of wing, that is semi semi-major and minor axis length of the ellipse.

$$\text{Area (A)} = \pi ab/4$$

Accordingly, $a = 0.5$ and $b = 0.32$ m

Referring to many research papers the maximum number of flaps the wing performed was 6. So, considering this the maximum angular velocity is obtained by

$$\omega = f \times 60 \times 0.10472$$

Radius (R) = Centroid of quarter ellipse

So the linear velocity required for drag force is given by below equation,

$$V = R \times \omega$$

Using the above equations we can calculate the drag force acting on a wing.

But there is 1 pair of wings so the total drag force would be 2 times. So total force would be the sum of total drag force and weight. Then the required torque would be this force into radius (distance from centroid).

$$\text{Total drag (Fd)} = 2 \times Fd$$

$$\text{Weight} = W$$

$$\text{Total force} = Fd + W$$

$$\text{Crank Radius} = r$$

$$\text{Torque} = (Fd + W) \times r$$

By looking at the available BLDC motors and feasible reduction ratio, a 1000KV BLDC motor and 22.8 reduction was selected.

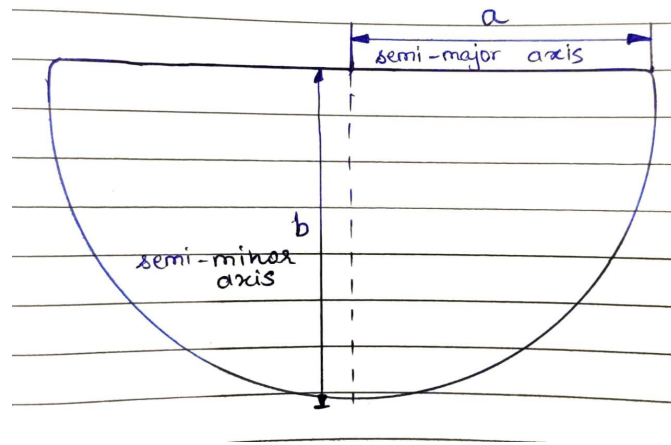


Figure 2: Wing Profile

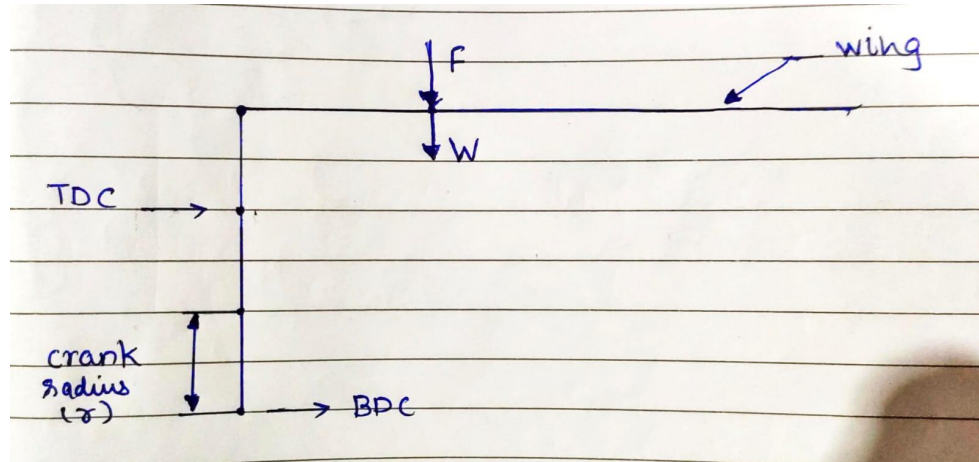


Figure 3: FBD of wing and crank

b. Servo Motor Torque calculation for Tail

Servo motor was used to actuate or rotate the tail in the vertical plane because of its inbuilt feedback mechanism, light weight, weight to torque characteristics and ease of control.

The forces acting on the tail are the same which acts on wings. Here the shape of the tail is an isosceles triangle and accordingly its area is calculated. The drag force and weight acts on the centroid of the triangle. The required torque would be this total force multiplied by the distance between the centroid of the triangle and servo shaft.

$$F_d = 1/2 \times C_d \times \rho \times A \times V$$

$$\text{Area (A)} = bh/2$$

$$\omega = \text{Rated speed of Servo}$$

$$\text{Radius (R)} = \text{Centroid of isosceles triangle}$$

$$\mathbf{V} = \mathbf{R} \times \boldsymbol{\omega}$$

$$\text{Torque} = (\mathbf{F}_d + \mathbf{W}) \times \mathbf{R}$$

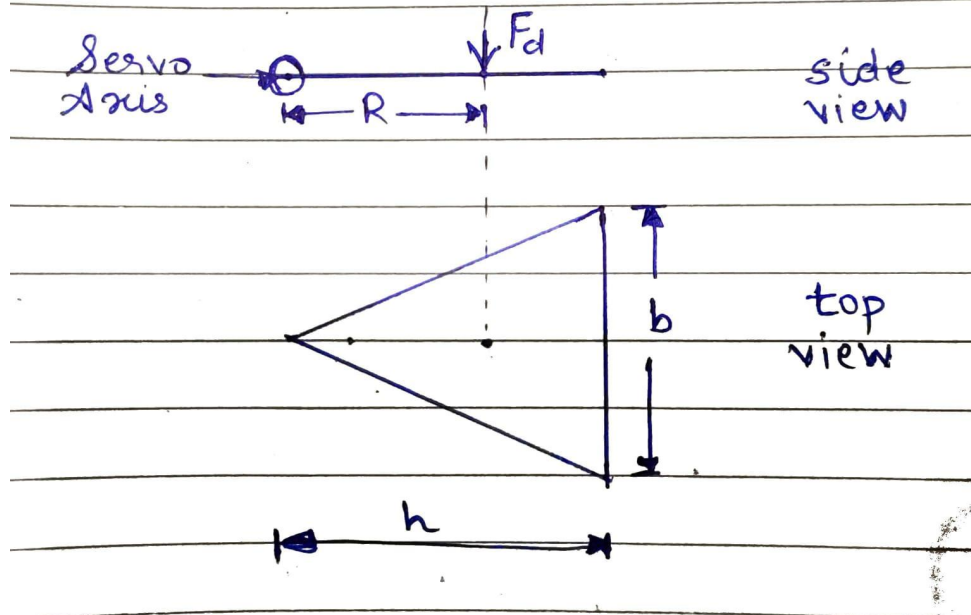


Figure 4: FBD of tail

For all the calculations, the density of air is taken 1.225 kg/m^3 and coefficient of drag is 1.05 for flat surfaces.

C. Gearbox Calculations:

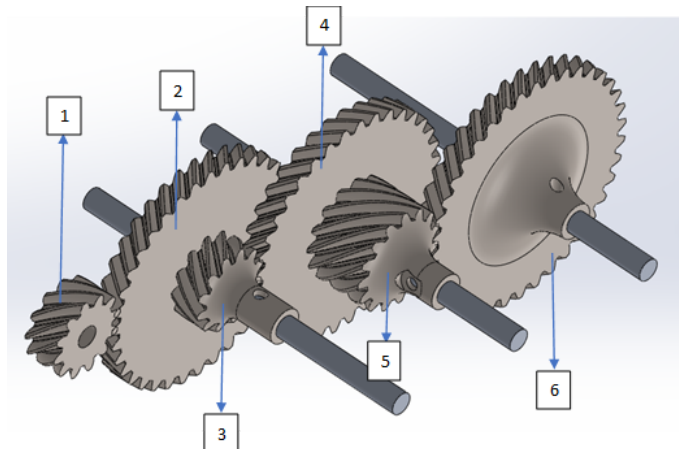


Figure 5: Gearbox

Table 1: Gear ratio calculations

Gear No.	No. of teeth	Total Reduction achieved
1 (Input Gear)	12	0
2	36	$36/12=3$
3	12	3 (Compound Gear)
4	36	$3 \times (36/12) = 9$
5	15	9 (Compound Gear)
6 (Output Gear)	38	$9 \times (38/15) = 22.8$

The input torque of the BLDC motor is around 1.5 kg cm. The required torque for flapping of the wing is 30 kg cm. The number of flaps required is around 4-6 flaps per second. So, considering both these factors an optimal reduction of 22.8 was calculated which will suffice required torque and flaps per second as well. The output torque comes out to be around 34 kgcm and the speed can be adjusted as per the requirement using the ESC for BLDC motor.

Gears manufactured earlier were spur gears, but the wear and tear, vibrations and loud sound made us try helical gears. Helical gears gave more efficient results with smooth transmission, less vibrations and less wear and tear. The number of teeth for gear no.1 is 12. The 2nd gear meshed with the first one has 36 teeth and so the reduction achieved here is $36/12=3$. Further a compound gear is attached to the same shaft having 12 teeth as well. This 3rd gear is further meshed with a 4th helical gear having 36 teeth again. The reduction now is calculated to be $3 \times (36/12) = 9$. Further a 5th compound gear is attached to this 5th gear having 15 teeth. This 5th gear is then meshed with 6th and final gear having 38 teeth. This equals the final reduction as $9 \times (38/15) = 22.8$.

d. Front pivot mechanism calculations

We have assumed here that when the crank is at the bottom dead center (lowest position)

the wing would be horizontal.

Considering this, a geometrical relationship between the flapping angle of wing, crank radius, center distance between rod end bearings and distance between rod end bearing and frontal pivot was established.

AP = Center distance between rod end bearings (d)

BP = Crank Diameter ($2r$)

OA = Distance between rod end bearing and frontal pivot (x)

$\angle \text{NOM}$ = Flapping angle of wing (θ)

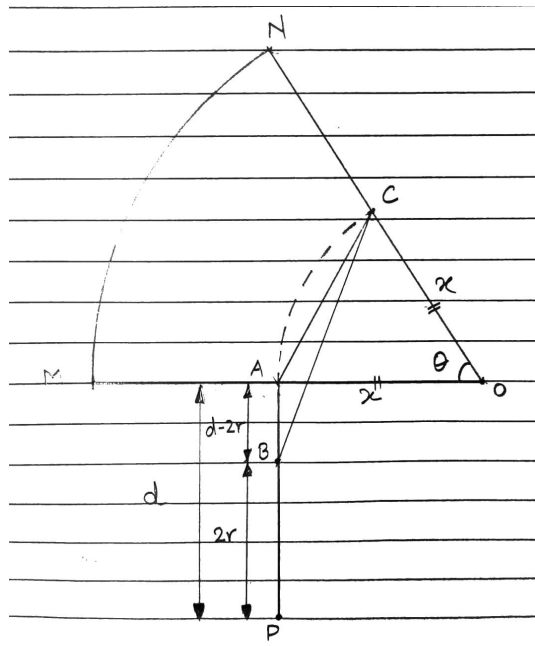


Figure 6: Front pivot geometry

OA = OB (Radius)

Applying sine rule to $\triangle OAB$

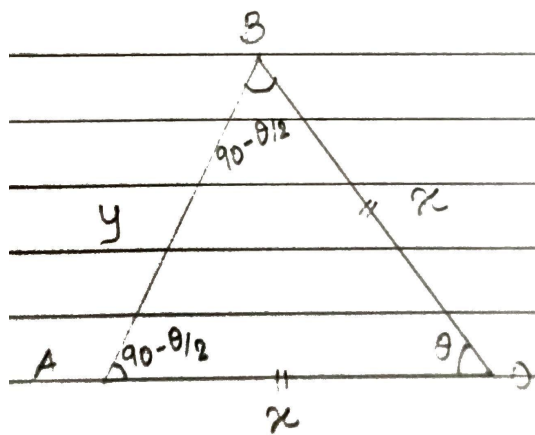


Figure 7: Front pivot geometry

$$\frac{\sin \theta}{y} = \frac{\sin(90 - \frac{\theta}{2})}{x}$$

$$y = x \frac{\sin \theta}{\cos \frac{\theta}{2}}$$

Assume flapping angle θ , we can calculate y (AB). Considering the design dimensions, x was assumed 23 mm

Now consider ΔABC , applying sine and cosine rule to ΔOAB ,

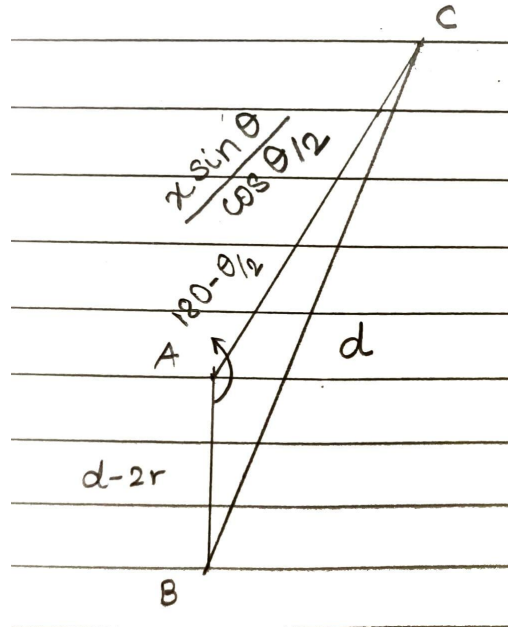


Figure 8: Front pivot geometry

$$\frac{\sin A}{a} = \frac{\sin B}{b} = \frac{\sin C}{c}$$

$$\frac{\sin(180 - \frac{\theta}{2})}{d} = \frac{\sin B}{x \frac{\sin \theta}{\cos \frac{\theta}{2}}} = \frac{\sin C}{d - 2r}$$

$$a = \sqrt{b^2 + c^2 - 2 \cdot b \cdot c \cdot \cos A}$$

Here,

$$d = \sqrt{y^2 + (d - 2r)^2 - 2 \cdot y \cdot (d - 2r) \cdot \cos(180 - \frac{\theta}{2})}$$

$$y = x \frac{\sin \theta}{\cos \frac{\theta}{2}}$$

By assuming flapping angle and d or (d-2r) we can find rest all of the values
By using these formulas, these are assumed and obtained values,

Parameter	Value
θ	600
x	23 mm
d	51.5 mm
r	11 mm

E. Design

1. Gearbox

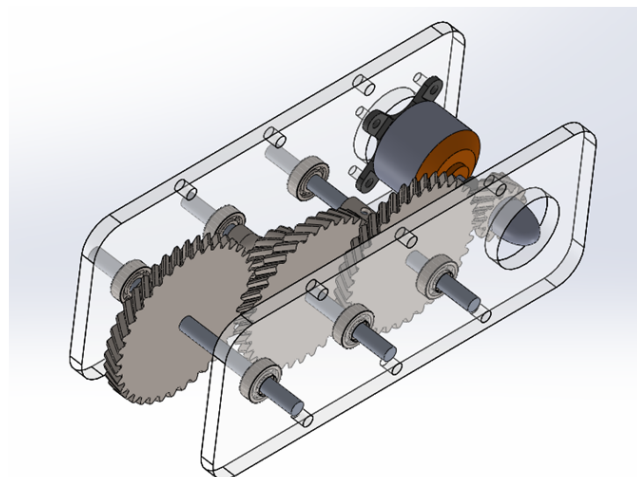


Figure 9: Gearbox

2. Frontal pivot mechanism

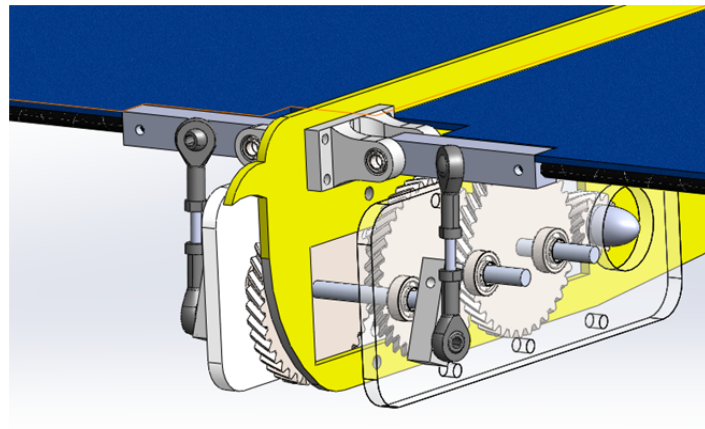


Figure 10: Front pivot mechanism

3. Back pivot

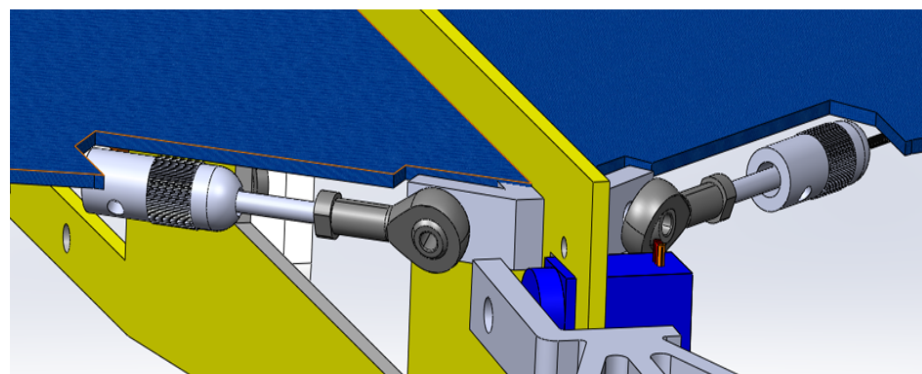
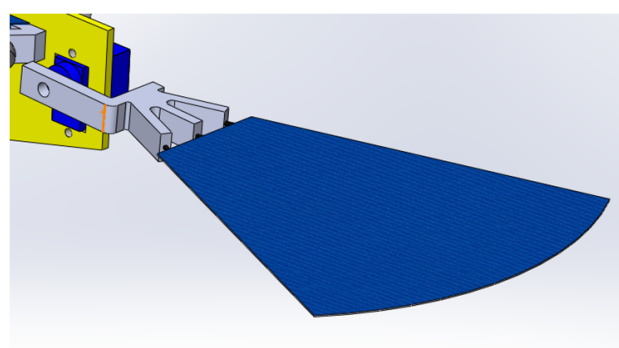


Figure 11: Back Pivot

4. Tail Mechanism



5. Final CAD

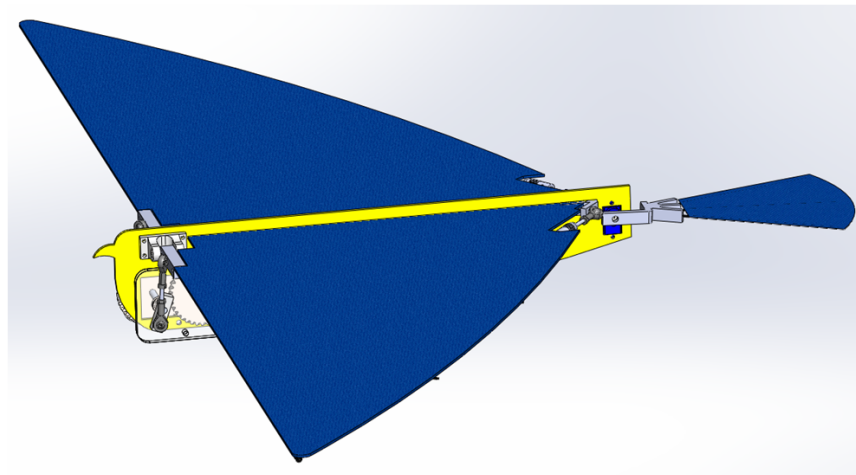


Figure 13: Final CAD

F. Analysis

1. Bearing Housing
 - a. **Material:** ABS
 - b. Material Properties

Properties of Outline Row 3: ABS					
	A	B	C	D	E
1	Property	Value	Unit	<input checked="" type="checkbox"/>	<input type="checkbox"/>
2	Density	1141	kg m ⁻³	<input type="checkbox"/>	<input type="checkbox"/>
3	Isotropic Elasticity			<input type="checkbox"/>	<input type="checkbox"/>
4	Derive from	Young's Mod...		<input type="checkbox"/>	<input type="checkbox"/>
5	Young's Modulus	1.19E+09	Pa	<input type="checkbox"/>	<input type="checkbox"/>
6	Poisson's Ratio	0.29		<input type="checkbox"/>	<input type="checkbox"/>
7	Bulk Modulus	9.4444E+08	Pa	<input type="checkbox"/>	<input type="checkbox"/>
8	Shear Modulus	4.6124E+08	Pa	<input type="checkbox"/>	<input type="checkbox"/>
9	Field Variables			<input type="checkbox"/>	<input type="checkbox"/>
13	Tensile Yield Strength	1.85E+07	Pa	<input type="checkbox"/>	<input type="checkbox"/>
14	Tensile Ultimate Strength	2.76E+07	Pa	<input type="checkbox"/>	<input type="checkbox"/>

Figure 14: Material Properties of ABS

c. Boundary Conditions

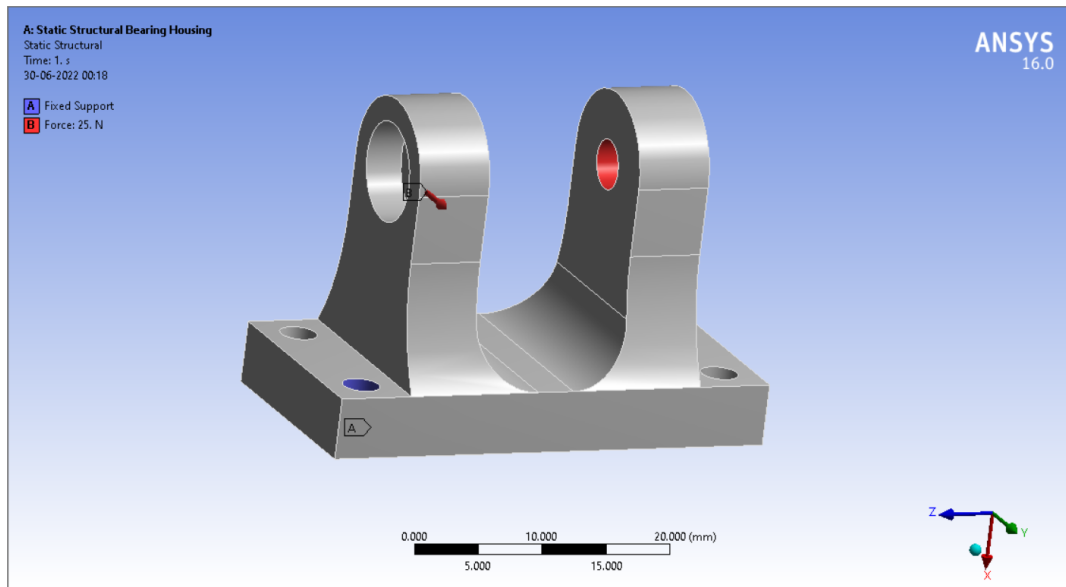


Figure 15: Boundary conditions of bearing housing

d. Results

I. Total Deformation

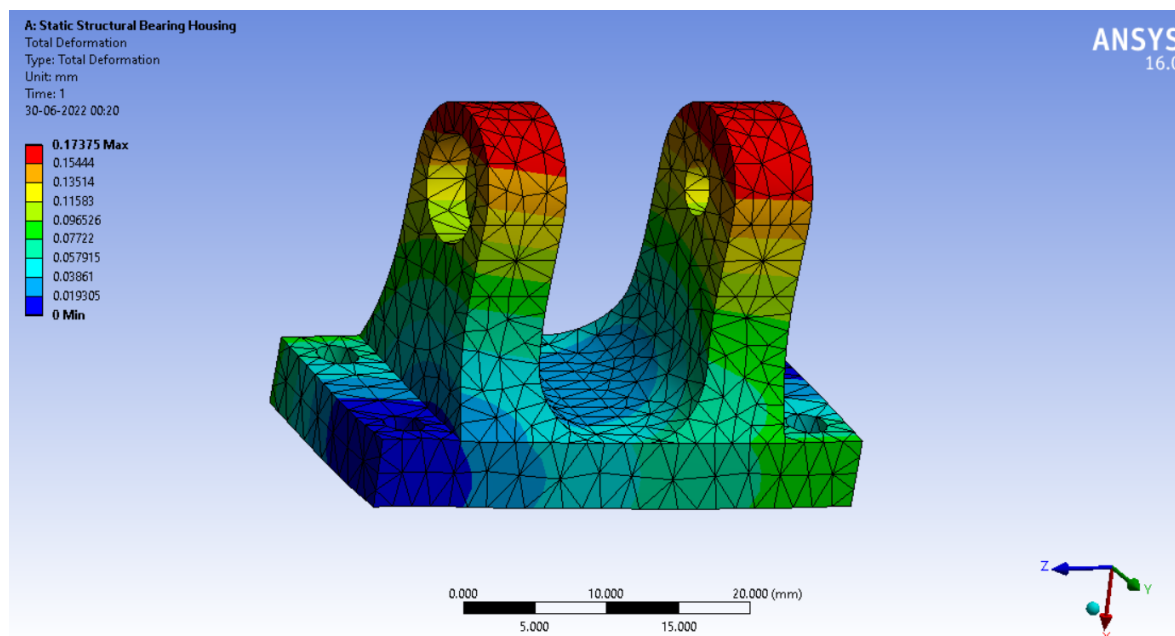


Figure 16: Equivalent Stress of Rod

II. Equivalent Stress

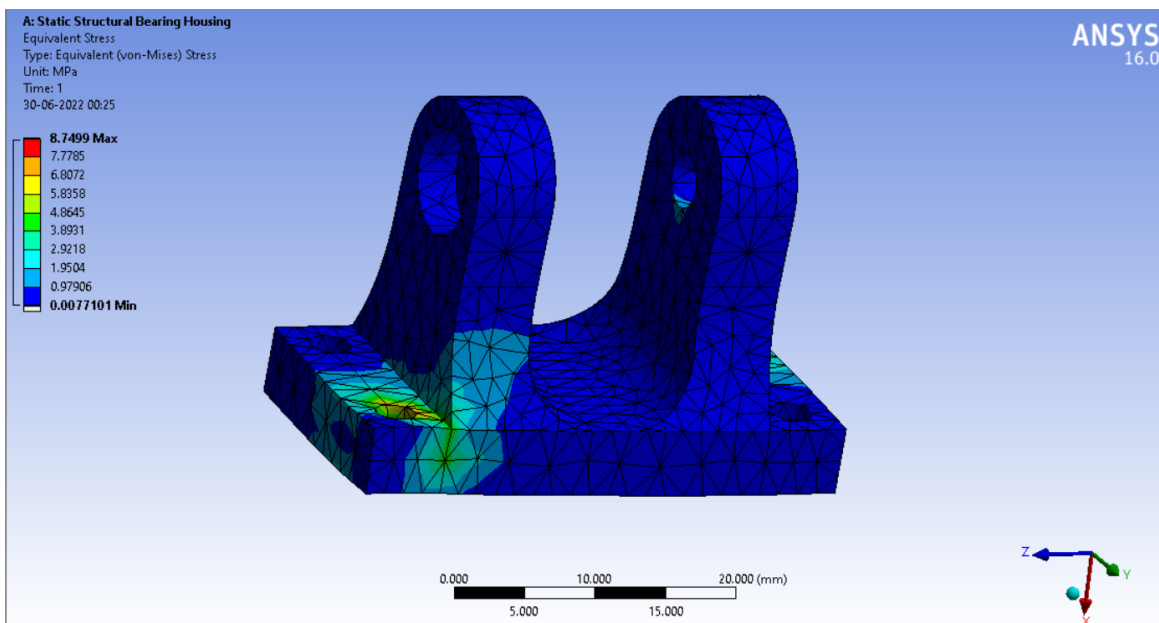


Figure 17: Equivalent Stress of Bearing Housing

2. Rod Connecting Link

- a. **Material:** ABS
- b. Material Properties

Properties of Outline Row 4: ABS 2					
	A	B	C	D	E
1	Property	Value	Unit	<input checked="" type="checkbox"/>	<input checked="" type="checkbox"/>
2	<input checked="" type="checkbox"/> Density	900	kg m ⁻³	<input type="checkbox"/>	<input type="checkbox"/>
3	<input checked="" type="checkbox"/> Isotropic Elasticity			<input type="checkbox"/>	<input type="checkbox"/>
4	Derive from	Young's Mod...		<input type="checkbox"/>	<input type="checkbox"/>
5	Young's Modulus	1.19E+09	Pa	<input type="checkbox"/>	<input type="checkbox"/>
6	Poisson's Ratio	0.29		<input type="checkbox"/>	<input type="checkbox"/>
7	Bulk Modulus	9.4444E+08	Pa	<input type="checkbox"/>	<input type="checkbox"/>
8	Shear Modulus	4.6124E+08	Pa	<input type="checkbox"/>	<input type="checkbox"/>
9	<input checked="" type="checkbox"/> Field Variables			<input type="checkbox"/>	<input type="checkbox"/>
13	<input checked="" type="checkbox"/> Tensile Yield Strength	1.85E+07	Pa	<input type="checkbox"/>	<input type="checkbox"/>
14	<input checked="" type="checkbox"/> Tensile Ultimate Strength	2.76E+07	Pa	<input type="checkbox"/>	<input type="checkbox"/>

Figure 18: Equivalent Stress of Rod

c. Boundary Conditions

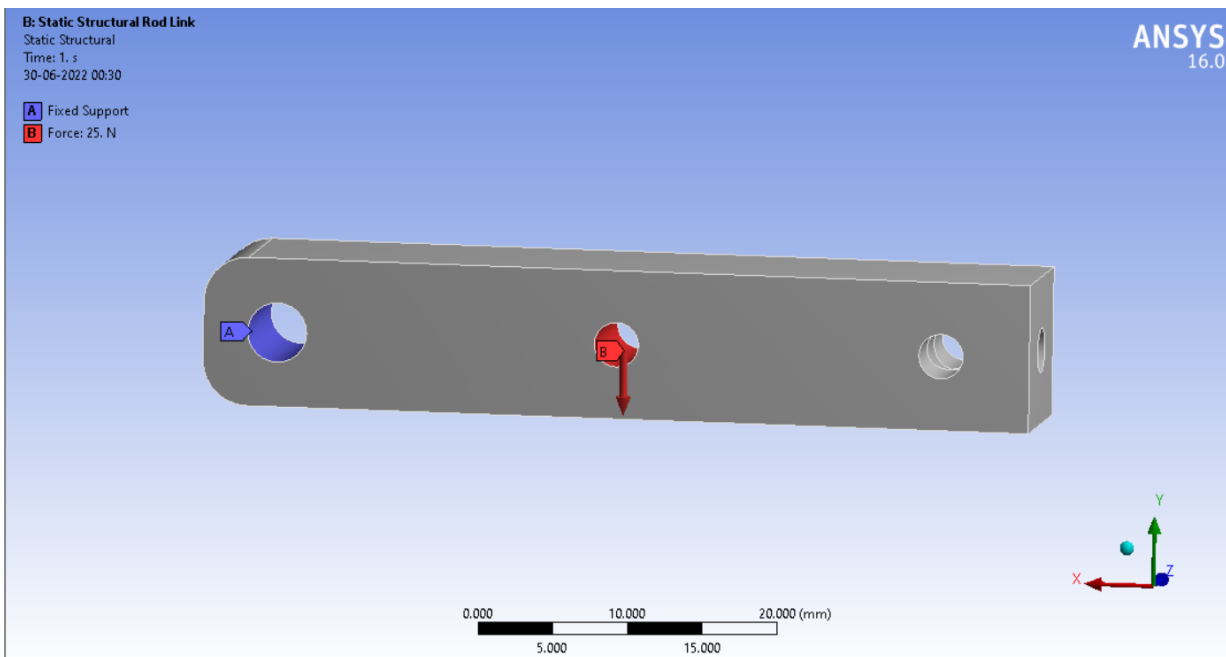


Figure 19: Boundary Condition of Rod Connecting Link

d. Results

I. Total Deformation

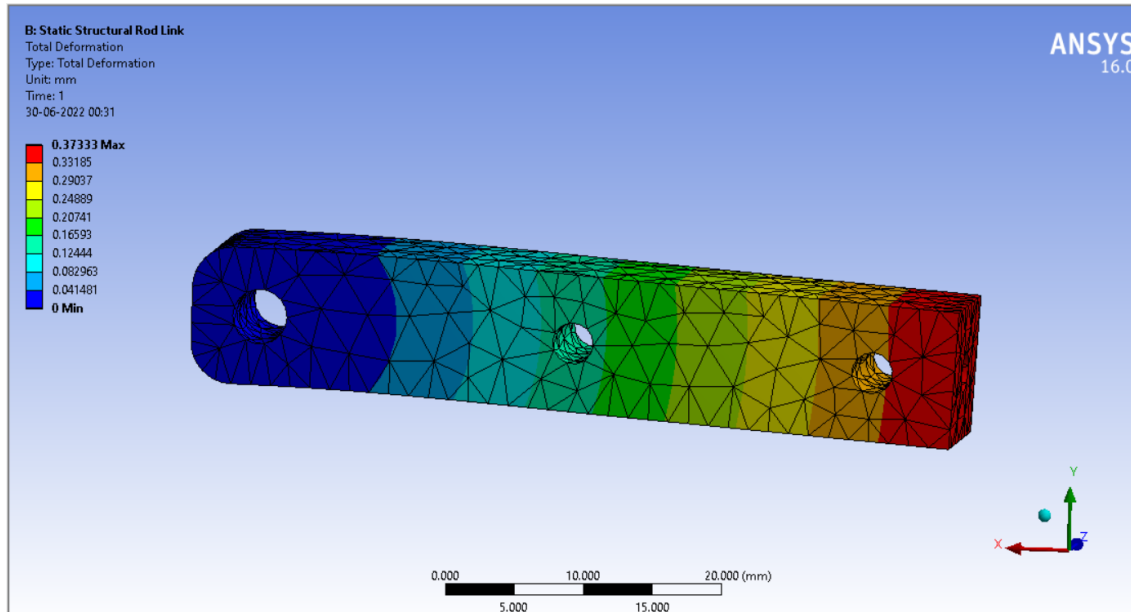


Figure 20: Total Deformation of Rod Connecting Link

II. Equivalent Stress

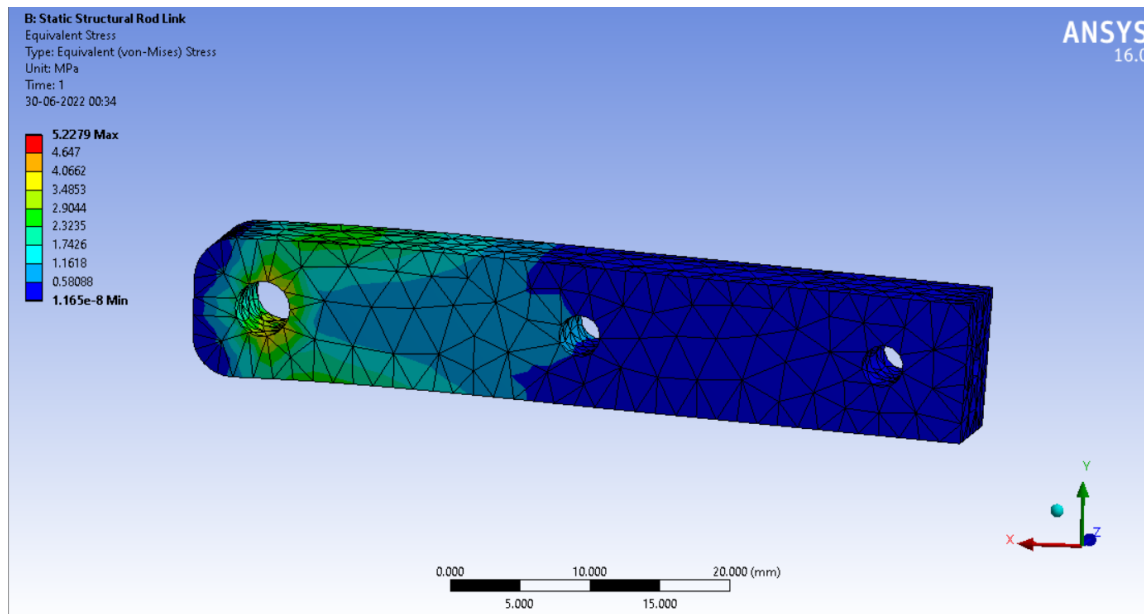


Figure 21: Equivalent Stress of Rod Connecting Link

3. Crank

- a. **Material:** ABS
- b. Material Properties

Properties of Outline Row 5: ABS 3				
	A	B	C	D E
1	Property	Value	Unit	<input checked="" type="checkbox"/> <input type="checkbox"/>
2	<input checked="" type="checkbox"/> Density	960	kg m ⁻³	<input type="checkbox"/> <input type="checkbox"/>
3	<input checked="" type="checkbox"/> Isotropic Elasticity			<input type="checkbox"/> <input type="checkbox"/>
4	Derive from	Young's Mod...		<input type="checkbox"/> <input type="checkbox"/>
5	Young's Modulus	1.19E+09	Pa	<input type="checkbox"/> <input type="checkbox"/>
6	Poisson's Ratio	0.29		<input type="checkbox"/> <input type="checkbox"/>
7	Bulk Modulus	9.4444E+08	Pa	<input type="checkbox"/> <input type="checkbox"/>
8	Shear Modulus	4.6124E+08	Pa	<input type="checkbox"/> <input type="checkbox"/>
9	<input checked="" type="checkbox"/> Field Variables			<input type="checkbox"/> <input type="checkbox"/>
13	<input checked="" type="checkbox"/> Tensile Yield Strength	1.85E+07	Pa	<input type="checkbox"/> <input type="checkbox"/>
14	<input checked="" type="checkbox"/> Tensile Ultimate Strength	2.76E+07	Pa	<input type="checkbox"/> <input type="checkbox"/>

Figure 22: Material Properties of Crank

c. Boundary Conditions

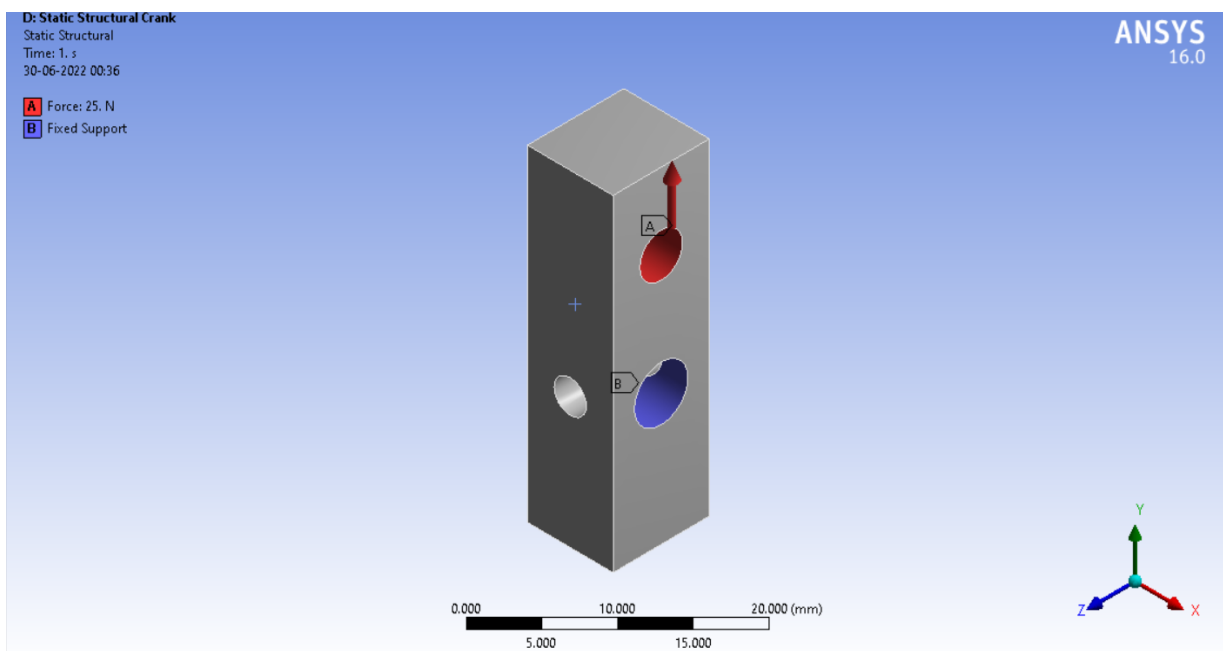


Figure 23: Boundary Conditions of Crank

d. Results

I. Total Deformation

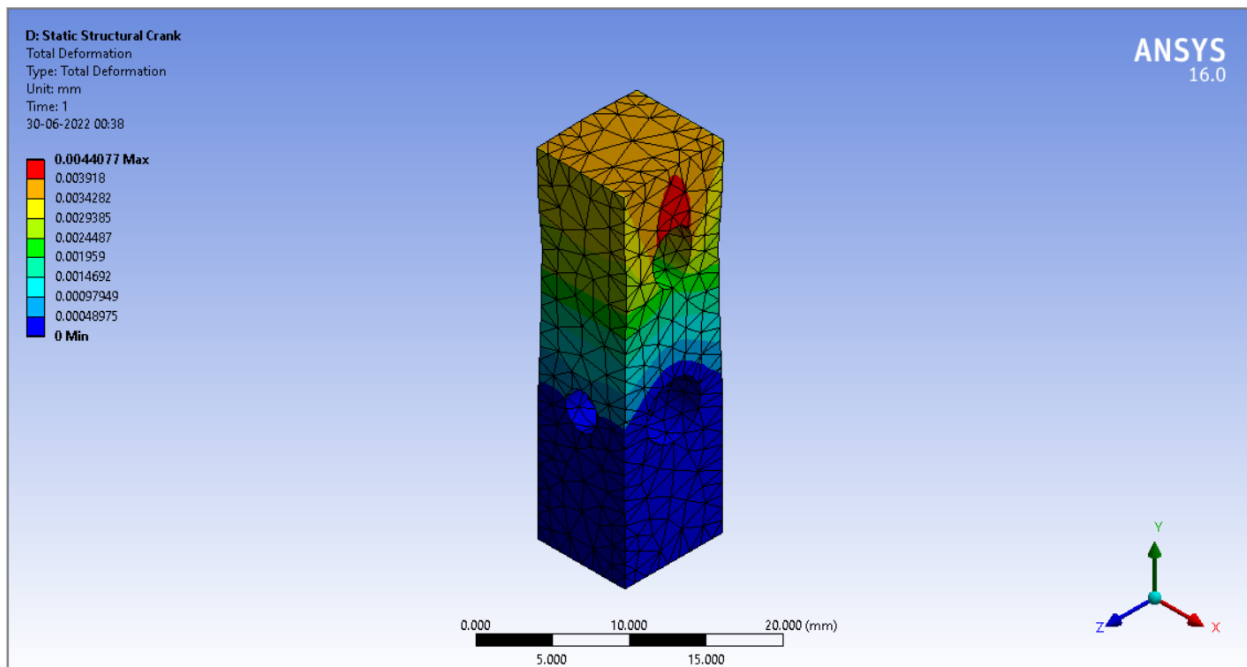


Figure 24: Total Deformation of Crank

II. Equivalent Stress

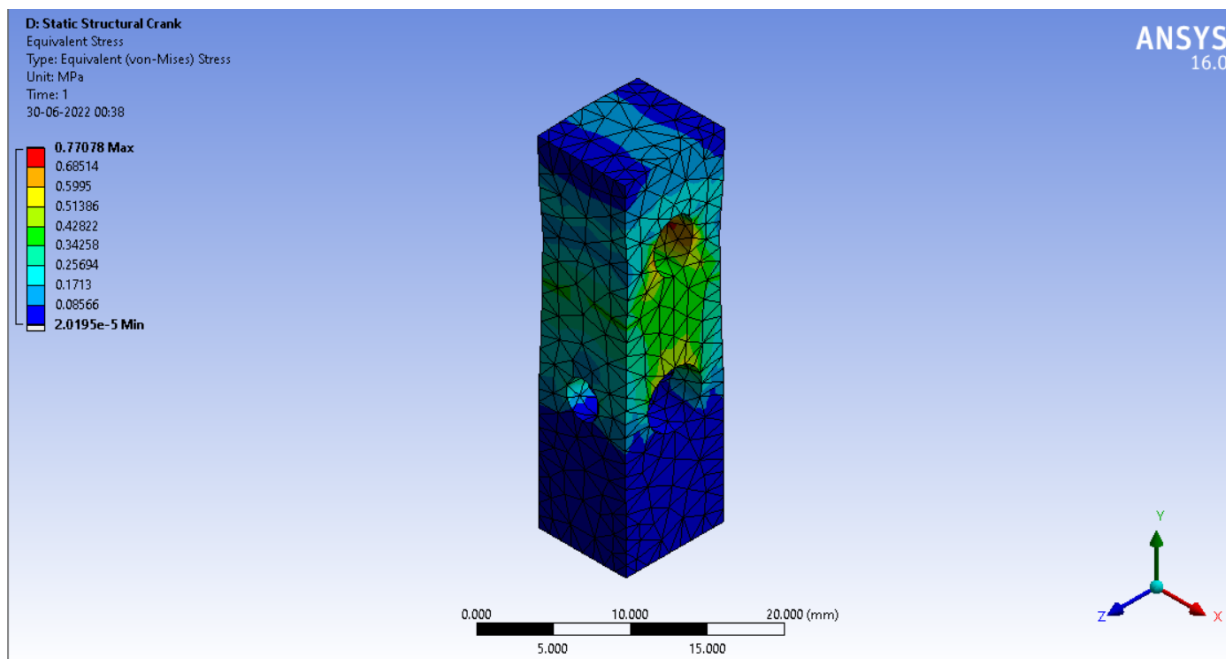


Figure 25: Equivalent Stress of Crank

4. Rod

- a. Material: SS
- b. Material Properties

Properties of Outline Row 4: Stainless Steel				
	A	B	C	D E
1	Property	Value	Unit	X P
2	Density	7750	kg m^-3	
3	Isotropic Secant Coefficient of Thermal Expansion			
4	Coefficient of Thermal Expansion	1.7E-05	C^-1	
5	Reference Temperature	22	C	
6	Isotropic Elasticity			
7	Derive from	Young's Mod...		
8	Young's Modulus	1.93E+11	Pa	
9	Poisson's Ratio	0.31		
10	Bulk Modulus	1.693E+11	Pa	
11	Shear Modulus	7.3664E+10	Pa	
12	Field Variables			
16	Tensile Yield Strength	2.07E+08	Pa	
17	Compressive Yield Strength	2.07E+08	Pa	
18	Tensile Ultimate Strength	5.86E+08	Pa	

Figure 26: Material Properties of Rod

c. Boundary Conditions

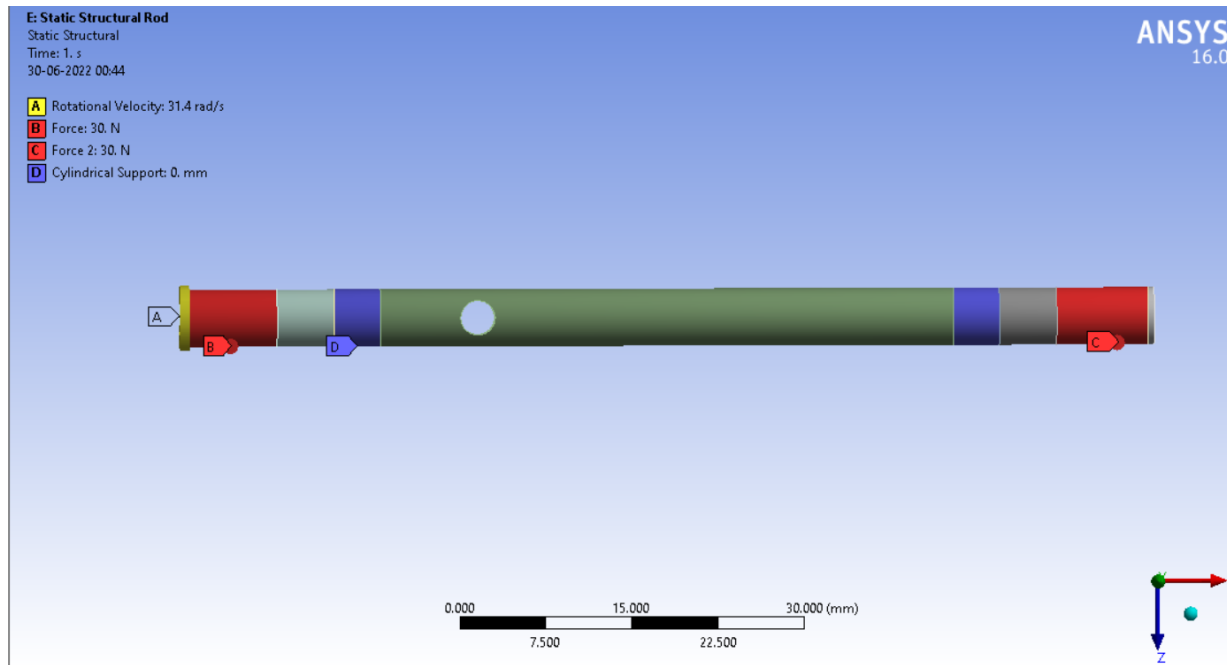
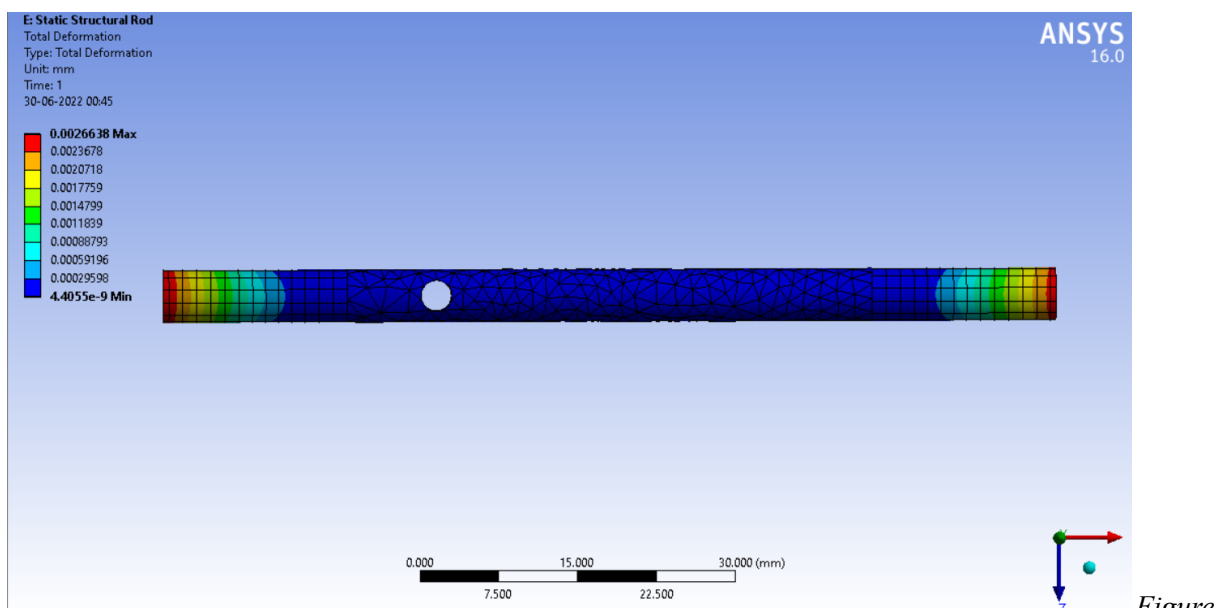


Figure 27: Boundary Conditions of Rod

d. Results

I. Total Deformation



28: Total Deformation of Rod

II. Equivalent Stress

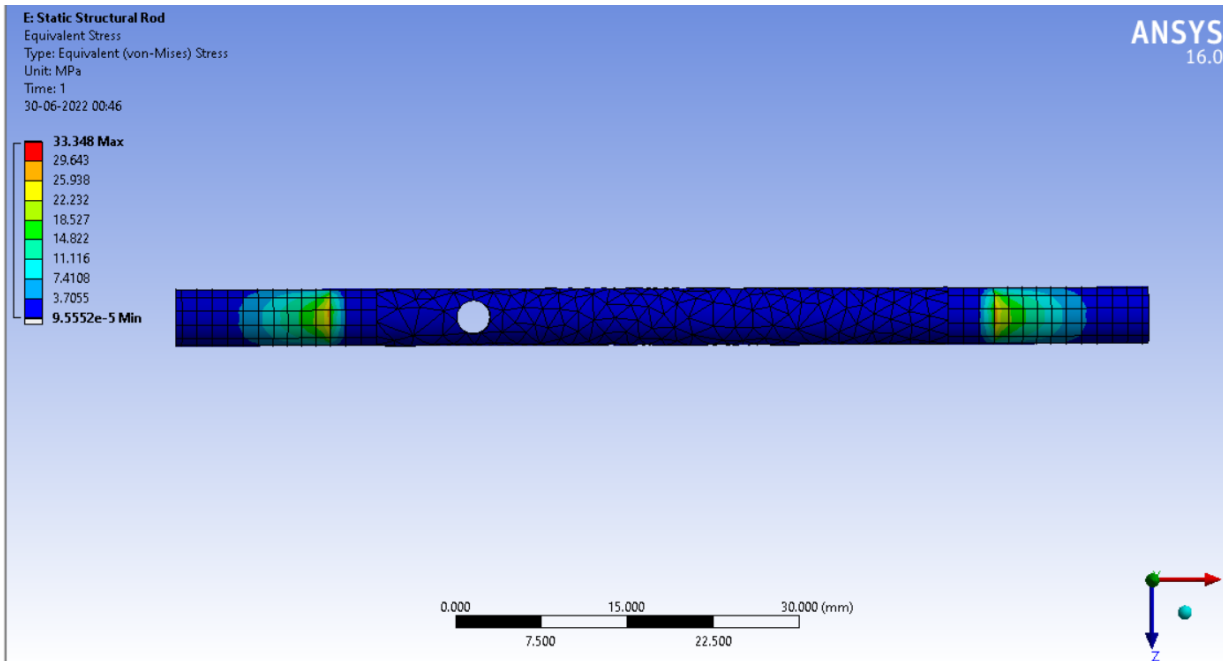


Figure 29: Equivalent Stress of Rod

G. Wing Flexibility

The flapping motion of the wings has to produce the upward lift as well as the forward thrust. To achieve this it is necessary that the wings are flexible and have a torsional movement about the wing span. There has to be a lag between the leading edge and the trailing edge of the wing during the flapping motion. During the downward stroke the angle of attack of the wing should be negative, that is the leading edge should be below the trailing edge. And during the upstroke the angle of attack should be positive. This can be achieved by having the appropriate design of the wing skeleton. This will lead to the generation of lift and thrust in the downward stroke and generation of thrust during the upward stroke

H. Materials

It was crucial to have the weight of the ornithopter as minimum as possible. To achieve this, it was decided to use composite materials which have higher strength to weight ratio. The main frame of the ornithopter has been made up of fiberglass Fr4. The skeleton of the wings has been made up of carbon fiber rods. The gears have been made up of ABS plastic. The wings have been made up of nylon fabric.

I. Manufacturing Processes

It was essential to manufacture the components accurately for proper assembly and smooth functioning of the ornithopter. Therefore advanced manufacturing processes have been employed in manufacturing the components. Water jet cutting machine has been used to cut the required profile of the fiberglass main frame. The gears have been made by the additive manufacturing process of 3d printing.

J. Electronics

1. Components

a) Arduino UNO:

The Arduino Uno is an open-source microcontroller board based on the Microchip ATmega328P microcontroller and developed by Arduino.cc. The board is equipped with sets of digital and analog input/output (I/O) pins that may be interfaced to various expansion boards (shields) and other circuits. The board has 14 digital I/O pins (six capable of PWM output), 6 analog I/O pins, and is programmable with the Arduino IDE (Integrated Development Environment), via a type B USB cable. It can be powered by the USB cable or by an external 9-volt battery, though it accepts voltages between 7 and 20 volts. It is similar to the Arduino Nano and Leonardo. The hardware reference design is distributed under a Creative Commons Attribution Share-Alike 2.5 license and is available on the Arduino website. Layout and production files for some versions of the hardware are also available.

The word "uno" means "one" in Italian and was chosen to mark the initial release of Arduino Software. The Uno board is the first in a series of USB-based Arduino boards; it and version 1.0 of the Arduino IDE were the reference versions of Arduino, which have now evolved to newer releases. The ATmega328 on the board comes pre programmed with a bootloader that allows uploading new code to it without the use of an external hardware programmer.

While the Uno communicates using the original STK500 protocol, it differs from all preceding boards in that it does not use the FTDI USB-to-serial driver chip. Instead, it uses the Atmega16U2 (Atmega8U2 up to version R2) programmed as a USB-to-serial converter.

- Microcontroller: ATmega328P
- Operating Voltage: 5V
- Input Voltage (recommended): 7-12V
- Inout Voltage (limit): 6-20V
- Digital I/O Pins: 14 (of which 6 provide PWM output)

- PWM Digital I/O Pins: 6
- Analog Input Pins: 6
- DC Current per I/O Pin: 20 mA
- DC current for 3.3V Pin: 50 mA
- Flash Memory: 32 KB (ATmega328P) of which 0.5 KB used by bootloader
- SRAM: 2 KB (ATmega328P)
- EEPROM: 1 KB (ATmega328P)
- Clock Speed: 16 MHz
- LED_BUILTIN: 13
- Length: 68.6 mm
- Width: 58.4 mm
- Weight: 25 g

b) Transceiver module NRF24L01

It uses the 2.4 GHz band and it can operate with baud rates from 250 kbps up to 2 Mbps. If used in open space and with lower baud rate its range can reach up to 100 meters. The module can use 125 different channels which gives a possibility to have a network of 125 independently working modems in one place. Each channel can have up to 6 addresses, or each unit can communicate with up to 6 other units at the same time.

The power consumption of this module is just around 12mA during transmission, which is even lower than a single LED. The operating voltage of the module is from 1.9 to 3.6V, but the good thing is that the other pins tolerate 5V logic, so we can easily connect it to an Arduino without using any logic level converters.

Three of these pins are for the SPI communication and they need to be connected to the SPI pins of the Arduino, but note that each Arduino board has different SPI pins. The pins CSN and CE can be connected to any digital pin of the Arduino board and they are used for setting the module in standby or active mode, as well as for switching between transmit or command mode. The last pin is an interrupt pin which doesn't have to be used.

c) Battery

1000mAh 4S 30C/60C Lithium polymer battery Pack (LiPo) batteries are equipped with heavy duty discharge leads to minimize resistance and sustain high current loads. Orange batteries stand up to the punishing extremes of aerobatic flight and RC vehicles. Each pack is equipped with gold plated connectors and JST-XH style balance connectors. All Orange Lithium Polymer battery packs are assembled using IR match cells.

- Model No: 1000/4S-30C
- Capacity : 1000 mAh.
- Weight:: 107 gm.
- Voltage : 14.8 V.
- Dimensions : 26 x 34 x 72(mm).
- Max Continuous Discharge : 30 C(30 A)

d) Electronic Speed Control

An ESC or an Electronic Speed Controller controls the brushless motor movement or speed by activating the appropriate MOSFETs to create the rotating magnetic field so that the motor rotates. The higher the frequency or the quicker the ESC goes through the 6 intervals, the higher the speed of the motor will be.

However, here comes an important question, and that's how do we know when to activate which phase. The answer is that we need to know the position of the rotor and there are two common methods used for determining the rotor position.

The first common method is by using Hall-effect sensors embedded in the stator, arranged equally 120 or 60 degrees from each other.

As the rotors permanent magnets rotate the Hall-effect sensors sense the magnetic field and generate a logic “high” for one magnetic pole or logic “low” for the opposite pole. According to this information the ESC knows when to activate the next commutation sequence or interval.

The term ESC stands for “electronic speed control is an electronic circuit used to change the speed of an electric motor, its route, and also to perform as a dynamic brake. These are frequently used on radio-controlled models which are electrically powered, with the change most frequently used for brushless motors providing an electronically produced 3-phase electric power low voltage source of energy for the motor.

An electronic speed controller can be designed with three essential components like a voltage regulator/ BEC (Battery Eliminator Circuit)), a Processor & the switching includes FETs. The BEC is a separation of the electronic speed control that will transmit power back to your receiver after that to servos.

This also includes one secondary function like when the motor is operated through a battery then

the motor gets its smallest voltage, then the BEC will keep some power for the flight control in dangerous situations so the motor doesn't consume total power from the battery. At present, the processor is completely enclosed within a single Si semiconductor chip.

e) BLDC Motor

As their name implies, brushless DC motors do not use brushes. With brushed motors, the brushes deliver current through the commutator into the coils on the rotor. So how does a brushless motor pass current to the rotor coils? It doesn't—because the coils are not located on the rotor. Instead, the rotor is a permanent magnet; the coils do not rotate, but are instead fixed in place on the stator. Because the coils do not move, there is no need for brushes and a commutator.

With the brushed motor, rotation is achieved by controlling the magnetic fields generated by the coils on the rotor, while the magnetic field generated by the stationary magnets remains fixed. To change the rotation speed, you change the voltage for the coils. With a BLDC motor, it is the permanent magnet that rotates; rotation is achieved by changing the direction of the magnetic fields generated by the surrounding stationary coils. To control the rotation, you adjust the magnitude and direction of the current into these coils.

A BLDC motor with three coils on the stator will have six electrical wires (two to each coil) extending from these coils. In most implementations three of these wires will be connected internally, with the three remaining wires extending from the motor body (in contrast to the two wires extending from the brushed motor described earlier). Wiring in the BLDC motor case is more complicated than simply connecting the power cell's positive and negative terminals; we will look more closely at how these motors work in the second session of this series. Below, we conclude by looking at the advantages of BLDC motors.

One big advantage is efficiency, as these motors can control continuously at maximum rotational force (torque). Brushed motors, in contrast, reach maximum torque at only certain points in the rotation. For a brushed motor to deliver the same torque as a brushless model, it would need to use larger magnets. This is why even small BLDC motors can deliver considerable power.

The second big advantage—related to the first—is controllability. BLDC motors can be controlled, using feedback mechanisms, to deliver precisely the desired torque and rotation speed. Precision control in turn reduces energy consumption and heat generation, and—in cases where motors are battery powered—lengthens the battery life.

BLDC motors also offer high durability and low electric noise generation, thanks to the lack of brushes. With brushed motors, the brushes and commutator wear down as a result of continuous moving contact, and also produce sparks where contact is made.

Electrical noise, in particular, is the result of the strong sparks that tend to occur at the areas where the brushes pass over the gaps in the commutator. This is why BLDC motors are often considered preferable in applications where it is important to avoid electrical noise.

f) Servo Motor

A servo motor is a type of motor that can rotate with great precision. Normally this type of motor consists of a control circuit that provides feedback on the current position of the motor shaft, this feedback allows the servo motors to rotate with great precision. If you want to rotate an object at some specific angles or distance, then you use a servo motor. It is just made up of a simple motor which runs through a servo mechanism. If a motor is powered by a DC power supply then it is called a DC servo motor, and if it is AC-powered motor then it is called an AC servo motor. For this tutorial, we will be discussing only the DC servo motor working. Apart from these major classifications, there are many other types of servo motors based on the type of gear arrangement and operating characteristics. A servo motor usually comes with a gear arrangement that allows us to get a very high torque servo motor in small and lightweight packages. Due to these features, they are being used in many applications like toy cars, RC helicopters and planes, Robotics, etc.

A servo consists of a Motor (DC or AC), a potentiometer, gear assembly, and a controlling circuit. First of all, we use gear assembly to reduce RPM and to increase torque of the motor. Say at initial position of servo motor shaft, the position of the potentiometer knob is such that there is no electrical signal generated at the output port of the potentiometer. Now an electrical signal is given to another input terminal of the error detector amplifier. Now the difference between these two signals, one comes from the potentiometer and another comes from other sources, will be processed in a feedback mechanism and output will be provided in terms of error signal. This error signal acts as the input for the motor and motor starts rotating.

Now the motor shaft is connected with the potentiometer and as the motor rotates so does the potentiometer and it will generate a signal. So as the potentiometer's angular position changes, its output feedback signal changes. After sometime the position of potentiometer reaches a position that the output of potentiometer is the same as the external signal provided. At this condition, there will be no output signal from the amplifier to the motor input as there is no difference between external applied signal and the signal generated at potentiometer, and in this situation the motor stops rotating.

g) Joystick Module

This module offers an affordable solution to that. The Joystick module is similar to analog joysticks found in gamepads. It is made by mounting two potentiometers at a 90 degrees angle. The potentiometers are connected to a short stick centered by springs. This module produces an output of around 2.5V from X and Y when it is in resting position. Moving the joystick will cause the output to vary from 0v to 5V depending on its direction. If you connect this module to a microcontroller, you can expect to read a value of around 512 in its resting position (expect small variations due to tiny imprecisions of the springs and mechanism) When you move the joystick you should see the values change from 0 to 1023 depending on its position.

2. Algorithm

There are two main tasks that have to be controlled wirelessly, the speed of the BLDC motor and the position of the servo motor. This is done with the help of radio frequency modules. The radio frequency transmitter module mounted on the controller sends the commands to the radio frequency receiver module located on the ornithopter. It has an operating frequency of 2.4 GHz. The Special Peripheral Interface (SPI) data protocol has been used for communication. Two joysticks communicate separately with the BLDC and the servo motor. The analog values sent to the receiver (0 to 1023) are mapped according to the range of the joystick module (-512 to 512). For the speed control of the BLDC motor, three specific speeds have to be achieved by sending three different values of PWM.. The range of the joystick module -512 to 512 is divided into 3 ranges, -512 to 20, 20 to 350 and 350 to 512 and three variables, namely D, M and F have been assigned to these ranges respectively. If the position of the joystick is between -512 to 20 then the variable D will be sent to the receiver module. In the receiver module, the three values of PWM 70,80 and 90 are assigned to the variables D,M and F respectively. So if the variable D is sent to the receiver module then a PWM of 70 will be sent to the BLDC motor. In the case of the servo motor, three specific angles have to be achieved. Again the range of the joystick module is divided into three ranges of -512 to -20, -20 to 20 and 20 to 512 and three variables, d,x and u have been assigned to these ranges respectively. If the position of the joystick is between -512 to 20 then the variable d will be sent to the receiver module. In the receiver module, the three values of shaft positions 70,130 and 180 are assigned to the variables d,x and u respectively. So if the variable d is sent to the receiver module then the angle of 70 degrees will be achieved by the servo motor.

K. Test Setup

1. Initial test setup:

The initial idea to verify the amount of lift generated was by using the moment balance theory. A lever was pivoted at its center and the ornithopter was placed at one end of it and a digital weight measuring device was attached at the other end. The lift generated by the ornithopter pulled one end of the lever upwards forcing the other end downwards. As the center point of the lever bisected the distance between the ornithopter and the weight measuring device, the amount of lift generated by the ornithopter was equal to the downwards force which was acting on the weight measuring device. The issue with this setup was that the readings were quite dynamic and instantaneous as the lift force changed continuously during flapping. Therefore it was not possible to record the readings.

$$F_{Lift} * r = F_d * r$$

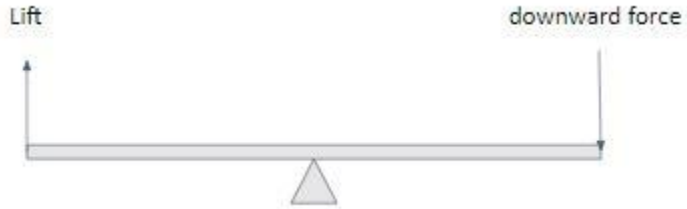


Figure 30: Forces Acting on Test Setup 1

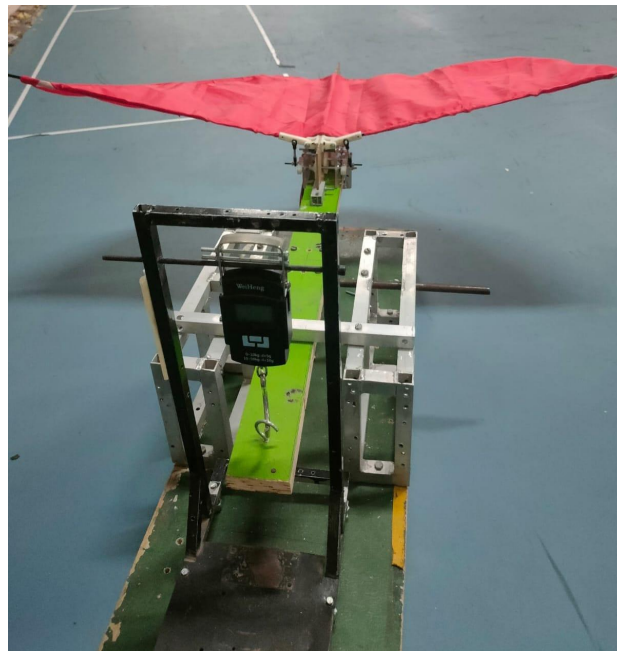


Figure 31: Test setup 1

2. Final phase test setup:

In the next test setup, the ornithopter was suspended using a rope from the ceiling. One end of the rope is attached to the ornithopter and the other end is to a hook attached to the ceiling. The position of attachment of rope on the ornithopter is determined visually such that the ornithopter remains stable when suspended without tilting in any direction. This setup does not provide any specific values such as lift force, thrust or speed but gives a general idea about the motion of the ornithopter. If the ornithopter is actuated and generates enough lift force, a visual slack would be seen in the rope concluding that the robot is producing enough lift force to lift itself up. We can also verify if the ornithopter will move forward or not using the same setup. If the ornithopter revolves in a circle such that the rope makes an angle theta () with vertical we can say that the ornithopter will definitely move forward if it was not suspended. Due to suspension the motion is

restricted and resultant motion achieved is a circular motion. The greater the angle theta the faster it will move forward.

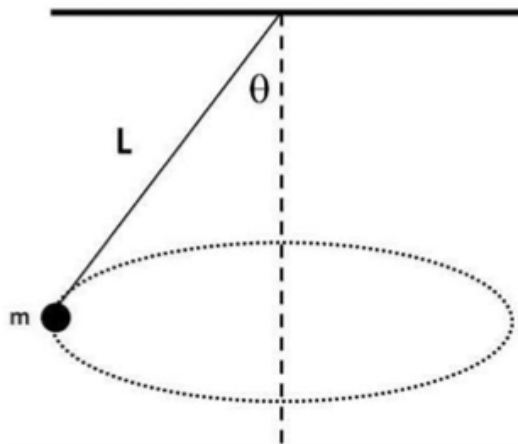


Figure 32: Test Setup 2

IV. Challenges faced:

Initially we faced difficulties in finding the required materials and components. We had to do an extensive market survey. Along with it most of the manufacturing processes employed were complex and time consuming like 3d printing which increased the project duration. Initially the teeth of 3d printed spur gears wore out quickly which were then replaced by helical gears. The flapping of wings is a dynamic system and hence it was difficult to perform the analysis. We also faced various issues regarding the electronics components and connections and it was difficult to troubleshoot these issues

V. Advantages of Ornithopter over drones

Ornithopters have a competitive advantage over other fixed-wing aircraft. Some of the advantages of ornithopters include their use as transport and surveillance vehicles. The ideal ornithopter would be able to perform everything a bird can. An ornithopter might take off almost vertically. This is related to the potential for flapping force. This would be extremely useful for observation vehicles, Navy aircraft carriers, and use in rugged terrain locations. The maneuverability of ornithopters far exceeds that of fixed-wing aircraft. Birds' agile dynamic motions may beat those of airplanes, allowing for better surveillance and employment in difficult circumstances. Ornithopters are capable of flying at low speeds. Fixed-wing aircraft would stall if flown below their limits, and expert pilots are required to handle maneuvers at low speeds without catastrophic outcomes. According to the research, flapping would not cause stalls and would only necessitate a modest increase in power requirements beyond the ideal values. Ornithopters have the potential to be more efficient than fixed-wing aircraft. The gliding process,

as well as the lower start time of the flapping engine when compared to jet and propeller engines, allows for a true glide as opposed to the cruise conditions reached by jet aircrafts.

VI. Future Scope:

The further extension of the project can be done in the way of aerial vehicles to spy or to monitor the areas where there are chances of occurrence of any hazard by attaching a camera and displaying the visuals in smart phone or screen. As Ornithopter is something that appears to be a part of nature there are less chances of identifying that they are being spied on. Hence these can be used in the army for many purposes. Taking this as the prototype we can develop aerial vehicles of huge size that can carry humans too.

VII. Applications:

1. Ornithopters can be made to resemble Birds or insects, they could be used for military applications without alerting the enemies that they are under surveillance.
2. Several ornithopters have been flown with video cameras on board, some of which can hover and maneuver in small spaces.

VIII. Conclusion:

Ornithopters have been a relatively obscure area of research in comparison to fixed wing aircraft and the field of ornithopter design is sparsely populated. We have chosen a suitable flapping mechanism to mimic the flapping action of the birds. Based on the approximate weight of the bird it was decided to mimic the buzzard bird. Wing area was calculated based on theory of wing loading. Suitable BLDC motor and the gear ratio value has been chosen to obtain a required force and flapping frequency. The Ornithopter has been designed and fabricated based on these inputs. All components have been designed to be as lightweight and high performance as possible so as to maximize payload capacity and are intended to fail in predictable and repairable ways. Examples of this are the screw in wing spars and replaceable faceplates. In addition to this all parts of the ornithopter are simple and inexpensive to fabricate and assemble. The ornithopter is wirelessly controlled with the help of a radio frequency module.

References

- [1] Sean Kinkade. Ornithopter. US Patent 9858922, May 17, 2001
- [2] Nathan Chronister. Ornithopter with independently controlled wings. US Patent 11147044
- [3] Robyn Lynn Harmon. “Aerodynamic modeling of a flapping membrane wing using motion tracking experiments.” Master’s thesis, University of Maryland
- [4] Bar-Cohen, Y. (2011). Biomimetics: nature-based innovation. CRC press
- [5] Berdeguer, C., Schmidtman, H., & Waid-Jones, A. (2015). Ornithopter Testbed to Discover Forces Produced by Flapping Wing Movement. Worcester Polytechnic Institute. Retrieved September 21, 2015.
- [6] Beando, A., Chung, J., Overton, C., Pietri, T., & Ramirez, K. (2014). Theoretical Model and Test Bed for the Development and Validation of Ornithopter Designs. Worcester Polytechnic Institute. Retrieved September 21, 2015.
- [7] Zachary John Jackowski, “Design and Construction of an Autonomous Ornithopter”, 2009
- [8] Jensen, M. (1956). Biology and physics of locust flight. III The aerodynamics of locust flight. Phil. Trans. R. Soc. Lond. B 239, 511-552
- [9] T. Weis-Fogh, Quick estimates of flight fitness in hovering animals, including novel mechanisms for lift production, J. Exp. Biol. 59, p.169-230.
- [10] Froude, R. E., “On the Part Played in Propulsion by Differences of Fluid Pressure,” Transactions of the Institution of Naval Architects, Vol. 30, pp. 390-409
- [11] Glauert, H., A General Theory of Autogyro, Research and Memoranda No. 1111, Scientific Research Air Ministry
- [12] Ellington, C. P., “The Aerodynamics of Hovering Insect Flight: V. A vortex theory.” Philos. Trans. R. Soc., London, Ser. B
- [14] Sane, S. P., “Review. The Aerodynamics of Insect Flight.” The Journal of Experimental Biology, 206, 2003, pp. 4191-4208
- [15] NPTEL course – “Physics of flight of Birds”

